

Surface-Enhanced Electric Intensities on Large Silver Spheroids

P. W. Barber

*Department of Electrical and Computer Engineering, Clarkson College of Technology,
Potsdam, New York 13676*

and

R. K. Chang

*Section of Applied Physics and Center for Laser Diagnostics, Yale University,
New Haven, Connecticut 06520*

and

H. Massoudi

Department of Electrical Engineering, University of Utah, Salt Lake City, Utah 84112

(Received 30 September 1982)

Electrodynamic calculations of the electric field on the surface of large Ag prolate spheroids indicate that the field enhancement decreases rapidly, the resonance shifts to longer wavelengths and broadens, and a new set of higher-order resonances appears at shorter wavelengths. These results form the basis for comparison with surface-enhanced Raman scattering measurements from lithographically produced Ag microstructures.

PACS numbers: 78.30.-j, 68.20.+t, 78.20.-e

Surface-enhanced Raman scattering (SERS) has been found experimentally to be most intense from Ag surfaces possessing some form of roughness or from the Ag microstructures themselves.¹ Several vastly different enhancement models have been proposed.^{1,2} Among the different models, the electromagnetic (EM) enhancement mechanism has received the most attention.

The EM model for an isolated metallic micro-object considers the large local EM fields produced at the surface when the incident-wave frequency (ω_i) is in resonance with the localized surface plasmons.³⁻⁵ The dipole oscillating at the Raman frequency (ω_s) can, in turn, polarize the metallic micro-object and, if ω_s is in resonance with the localized surface plasmons, the micro-object can enhance the inelastic radiation reaching the detector.³⁻⁵ If the EM intensity enhancement factor at the surface is $L^2(\omega)$, then the overall enhancement for the detected SERS intensity is approximately $L^2(\omega_i)L^2(\omega_s)$. Another source for EM field enhancement occurs near a surface of high curvature. This "lightning rod effect" and the surface-plasmon resonance can in general occur simultaneously, resulting in very large enhancement for Raman molecules adsorbed at and near the tips of spheroids⁶ or hemispheroids.⁷ Thus far, only the electrostatic solution (which assumes that the particle is much smaller than the incident wavelength) has been used to calculate $L^2(\omega)$ for microstructures other

than Ag spheres.

Experimental investigation of the EM enhancement by Ag micro-objects requires extremely well characterized morphology. The most successful result for producing Ag microstructures of uniform shape, equal size, and large separation has been achieved with UV laser lithography.⁸ Scanning electron micrographs revealed that these Ag microstructures are to the first approximation prolate spheroids with 3:1 and 2:1 axial ratios and the semiminor axis $b \approx 50$ nm. The following series of significant measurements have been performed on these microstructures: (1) the wavelength dispersion of the SERS from adsorbed C≡N complexes with the entire microstructure surrounded in several homogeneous media⁸—air, water, and cyclohexane; (2) surface-enhanced second-harmonic generation from the Ag microstructures⁹; and (3) surface-influenced absorption and luminescence of adsorbed dye molecules.¹⁰ These experimental results indicate that the linewidths of these resonances are some 15 times wider and the enhancement factors are much less than those predicted by the electrostatic solution.⁸ On the other hand, the influence of different surrounding media on the wavelength dependence of the SERS intensity was qualitatively in accordance with the electrostatic spheroid calculations.⁸

The much wider surface-plasmon linewidth could be reconciled either by assuming an extraordinarily large value for the imaginary part

of $\epsilon(\omega)$ for Ag or by assuming a distribution of axial ratios ($a:b$) in the electrostatic solution.⁸ The electrostatic calculations were recently modified¹¹ by including (1) additional electron scattering loss when the minor axis is less than the electron mean free path in the bulk, and (2) radiative energy losses at and near the tips of the spheroids as the size is increased. The inclusion of radiation damping decreases the electrostatic $L^2(\omega)$ and gives a calculated linewidth and line shape which are more in agreement with the experimental results. However, all of these calculations were still based on electrostatic solutions for the EM fields. For the lithographically produced Ag particles with $a = 100$ nm (2:1 spheroids) and $a = 150$ nm (3:1 spheroids) and for wavelengths in the visible region, a/λ_0 is well outside the validity range of the electrostatic solution.¹²

This paper reports the first electrodynamic calculations of the electric field enhancement at the surface of prolate spheroidal Ag particles. The electrodynamic results are exact and impose no restriction on particle size. However, these calculations are computer intensive. Bulk dielectric constants for Ag (Johnson and Christy¹³) and an isolated prolate spheroid are assumed. Only the case with the incident field polarized parallel to the long axis of the spheroid is considered, since this polarization results in the greatest surface fields.

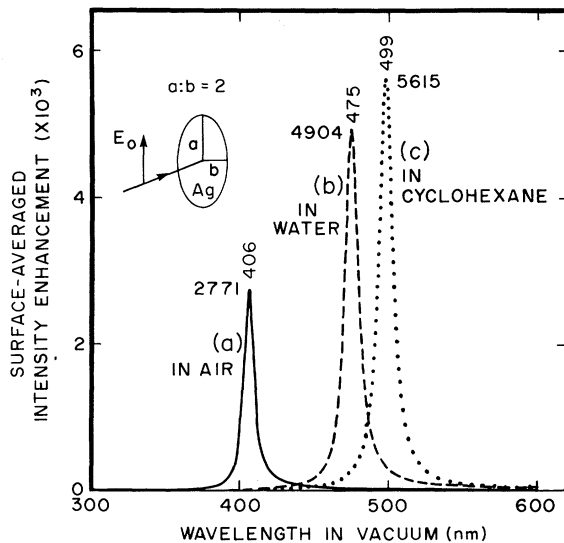


FIG. 1. $L^2(\omega)$ calculated in the electrostatic limit for a 2:1 Ag prolate spheroid embedded in (a) air ($\epsilon_m = 1.0$); (b) water ($\epsilon_m = 1.77$); and (c) cyclohexane ($\epsilon_m = 2.04$).

In the electrostatic solution, the electric field inside the spheroid, E_{in} , is a function of $\epsilon(\omega)$ and ϵ_m , the dielectric constants of the metal and surrounding medium, respectively, and of A_z , the geometry-dependent depolarization factors.^{14,15} E_{in} is size independent and is greatly enhanced at the localized surface-plasmon resonance when $\epsilon(\omega) = \epsilon_m(1 - 1/A_z)$. Figure 1 shows $L^2(\omega)$ for a Ag spheroid in air ($\epsilon_m = 1$), water ($\epsilon_m = 1.77$), and cyclohexane ($\epsilon_m = 2.04$). With increasing ϵ_m or $a:b$, the surface-plasmon resonance shifts to longer wavelengths and $L^2(\omega)$ becomes larger.^{6,8}

There are two approaches in making electrodynamic calculations of the surface fields for larger spheroidal particles. The conventional approach separates the electromagnetic wave equation in spheroidal coordinates.¹⁶ By this method, light-scattering results have been obtained for large (a/λ_0 up to 3) prolate and oblate spheroids^{17,18} and for absorbing spheroids.¹⁹ Another method, called the T -matrix method, is applicable to arbitrarily shaped objects although it is usually restricted to bodies of revolution to simplify the mathematical problem.²⁰⁻²³ Electrodynamic calculations for large Ag spheroids require a large mainframe computer, in this case a Control Data 7600, and the indicated computation times refer to this machine. Although these results are for the surface-averaged enhancement, we have also calculated $|E|^2$ at different zones on the surface for a number of large

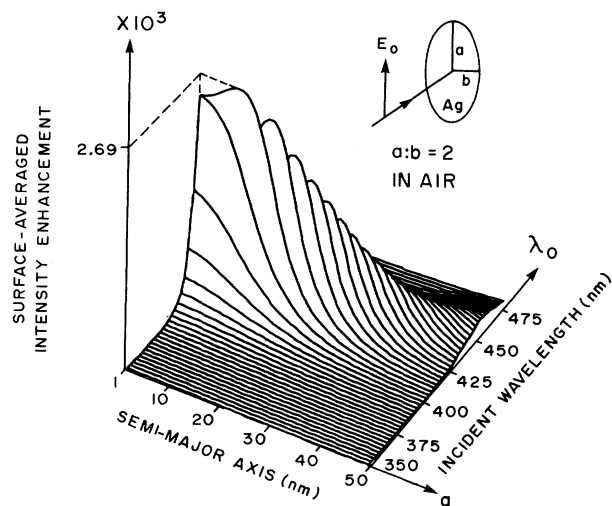


FIG. 2. $L^2(\omega)$ calculated with electrodynamic solution for a 2:1 Ag prolate spheroid embedded in air as a function of semimajor axis dimension and of incident wavelength.

spheroids²⁴ and found that $|E|^2$ is largest at the tip and decreases rapidly toward the equator, analogous to the electrostatic solution.

The size-wavelength dependence of $L^2(\omega)$ for a 2:1 prolate spheroid in air is shown in Fig. 2. This electrodynamic calculation required 67 min central processor unit (CPU) time. The maximum $L^2(\omega)$ is 2690 and occurs for $a = 8$ nm and $\lambda_0 = 407.5$ nm. With finer increments for a and λ_0 , the maximum $L^2(\omega)$ is 2730 and occurs at $a = 4$ nm and $\lambda_0 = 406.5$ nm. Electrodynamic calculations at $\lambda_0 = 406$ nm (the peak of the electrostatic solution in Fig. 1) for $a = 1$ nm and $a = 0.5$ nm give almost identical results of 2719 and 2720, respectively. This size independence of $L^2(\omega)$ confirms the validity of the electrostatic solution for $a = 1$ nm and less. The $\sim 2\%$ difference between 2719 (calculated by the T -matrix method for $a = 1$ nm) and 2771 (calculated by the electrostatic solution) is attributed to the numerical integration which is used in both procedures to calculate the surface average.

As the size is increased, these characteristics are evident from Fig. 2: (1) The major peak shifts to longer wavelengths; (2) $L^2(\omega)$ decreases rapidly from the electrostatic value; and (3) the linewidth of the $L^2(\omega)$ peak becomes broader (the Q decreases). These last two results are associated with multipole contributions and phase retardation which tend both to decrease $L^2(\omega)$ and to broaden the linewidth.

In order to compare the electrodynamic calculations with the experimental results for the wavelength dependence of the SERS intensity, we calculated the wavelength dependence for 2:1 spheroids with $a = 100$ nm and embedded in three different media: air, water, and cyclohexane. These electrodynamic calculations, which are shown in Fig. 3, required 80 min CPU time.

The calculated wavelength dependence for $\epsilon_m = 1$ consists of a broad peak at 630 nm and a considerably narrower peak at 365 nm. The broad peak is a continuation of the dipolar surface-plasmon resonance observed in Fig. 2. The narrow peak represents higher-order (multipole) surface-plasmon resonances. Compared with the experimental SERS results,⁸ several features should be noted: (1) The SERS is maximum at $\lambda_0 = 500$ nm and the calculated curve is maximum at $\lambda_0 = 630$ nm, both occurring at longer wavelengths than predicted by the electrostatic solution; (2) the linewidth for the SERS peak is ~ 100 nm while that for the calculated peak is ~ 250 nm; (3) both line shapes are asymmetrical, with a more grad-

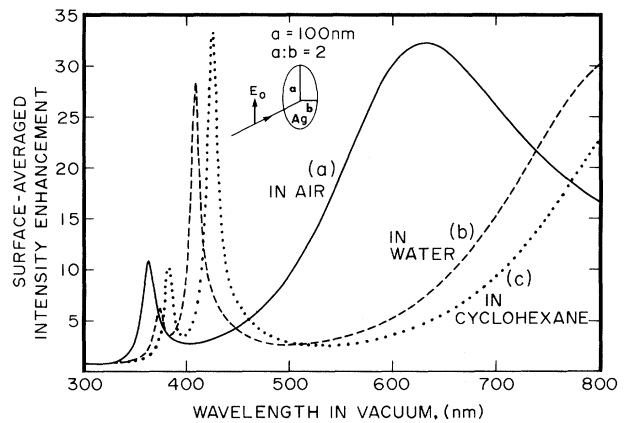


FIG. 3. The wavelength dependence of $L^2(\omega)$ for a 2:1 Ag prolate spheroid with semimajor axis $a = 100$ nm embedded in (a) air, (b) water, and (c) cyclohexane. Note the low value for $L^2(\omega)$.

ual decrease for the longer wavelength side; and (4) SERS was not measured below 458 nm; therefore, the existence of the calculated higher-order surface-plasmon resonance cannot be experimentally verified.

Upon considering immersion of the spheroids in water or in cyclohexane, the calculated wavelength dependences of $L^2(\omega)$ changed, as shown in Fig. 3. The broad $L^2(\omega)$ peak shifts to longer wavelengths upon change of the surrounding medium from air to water to cyclohexane, qualitatively similar to the experimentally observed SERS wavelength dependence.⁸ Figure 3 shows that another set of rather sharp surface-plasmon resonances occurs with comparable strength at shorter wavelengths. When the resonant peaks are so narrow, the SERS excitation profile is expected to exhibit two distinct peaks, one when λ_0 is coincident with the surface-plasmon peak and another when the Raman wavelength is coincident with the surface-plasmon peak. The calculation for the incident and reradiation waves has been solved only in the electrostatic limit.²⁵

On the basis of our electrodynamic calculations, we conclude that the effects of increasing the size of the Ag spheroids are (1) greatly reduced enhancement; (2) much broader and asymmetrical $L^2(\omega)$ line shapes, peaking at longer wavelengths; and (3) occurrence of a new set of multipole $L^2(\omega)$ peaks of narrower linewidth near the wavelength of the electrostatic solution peak, which can form a unique criterion for future experiments to test the validity of the electromagnetic model. Surprisingly, deviation from the electrostatic results occurred even when $a \approx 0.02\lambda_0$. The modified

electrostatic solution, which includes radiation damping as the first-order correction, is reasonably successful in predicting the dipolar resonance characteristics but fails to predict the higher-order resonances from multipole contributions. Detailed comparisons of our electrodynamic results and existing SERS excitation measurements on these Ag microstructures⁸ are not warranted as we neglected the coupling among neighboring spheroids at 300 nm away, the inhomogeneous surrounding caused by the SiO₂ posts, and possibly smaller microstructures on the Ag spheroids caused by the HCN vapor. Furthermore, these microstructures may only be approximated by a spheroid because the Ag was evaporated on cone-shaped SiO₂ posts. Nevertheless, our results indicate that the dimensions of these lithographically produced Ag microstructures are too large to give rise to enormous $L^2(\omega)$ as estimated from the electrostatic solution. Electrodynamical calculations for isolated and large Au and Pt spheroids are proceeding.

The authors thank Dr. G. C. Salzman of the Los Alamos National Laboratory for helpful discussions on computational techniques and gratefully acknowledge the partial support of this work by the National Science Foundation under Grants No. CPE 81-16087 and No. CPE 81-12835.

¹For a review of this subject, see *Surface Enhanced Raman Scattering*, edited by R. K. Chang and T. E. Furtak (Plenum, New York, 1982).

²T. E. Furtak and J. Reyes, *Surf. Sci.* **93**, 35 (1980).

³E. Burstein, Y. J. Chen, and S. Lundqvist, *Bull. Am. Phys. Soc.* **23**, 30 (1978); E. Burstein, C. Y. Chen, and S. Lundqvist, in *Proceedings of the USA-USSR Symposium on Light Scattering in Solids*, edited by J. L. Birman, H. Z. Cummins, and K. K. Rebane (Plenum, New York, 1979), p. 479.

⁴M. Moskovits, *J. Chem. Phys.* **69**, 4159 (1978), and *Solid State Commun.* **32**, 59 (1979).

⁵S. L. McCall, P. M. Platzman, and P. A. Wolff, *Phys. Lett.* **77A**, 381 (1980).

⁶J. I. Gersten, *J. Chem. Phys.* **72**, 5779, 5780 (1980); J. I. Gersten and A. Nitzan, *J. Chem. Phys.* **73**, 3023 (1980), and in *Surface Enhanced Raman Scattering*, edited by R. K. Chang and T. E. Furtak (Plenum, New York, 1982), p. 89; P. C. Das and J. I. Gersten, *J. Chem. Phys.* **76**, 3177 (1982).

⁷F. J. Adrain, *Chem. Phys. Lett.* **78**, 45 (1981).

⁸P. F. Liao, J. G. Bergman, D. S. Chemla, A. Wokaun, J. Melngailis, A. M. Hawryluk, and N. P. Economou, *Chem. Phys. Lett.* **82**, 355 (1981); P. F. Liao, in *Surface Enhanced Raman Scattering*, edited by R. K. Chang and T. E. Furtak (Plenum, New York, 1982), p. 379.

⁹A. Wokaun, J. G. Bergman, J. P. Heritage, A. M. Glass, P. F. Liao, and D. H. Olson, *Phys. Rev. B* **24**, 849 (1981).

¹⁰A. M. Glass, P. F. Liao, J. G. Bergman, and D. H. Olson, *Opt. Lett.* **5**, 368 (1980).

¹¹A. Wokaun, J. P. Gordon, and P. F. Liao, *Phys. Rev. Lett.* **48**, 957, 1574 (1982).

¹²M. Kerker, *The Scattering of Light and Other Electromagnetic Radiation* (Academic, New York, 1969), p. 84.

¹³P. B. Johnson and R. W. Christy, *Phys. Rev. B* **6**, 4370 (1972).

¹⁴J. A. Stratton, *Electromagnetic Theory* (McGraw-Hill, New York, 1941), p. 212.

¹⁵E. C. Stoner, *Philos. Mag.* **36**, 803 (1945).

¹⁶S. Asano and G. Yamamoto, *Appl. Opt.* **14**, 29 (1975).

¹⁷S. Asano, *Appl. Opt.* **18**, 712 (1979).

¹⁸S. Asano and M. Sato, *Appl. Opt.* **19**, 962 (1980).

¹⁹R. W. Schaefer, Ph.D. thesis, State University of New York at Albany, 1980 (unpublished).

²⁰P. C. Waterman, *Alta Freq.* **38** (Speciale), 348 (1969), and *Phys. Rev. D* **3**, 825 (1971), and *J. Appl. Phys.* **50**, 4550 (1979).

²¹*Acoustic, Electromagnetic and Elastic Wave Scattering—Focus on the T-Matrix Approach*, edited by V. K. Varadan and V. V. Varadan (Pergamon, New York, 1980).

²²P. W. Barber and C. Yeh, *Appl. Opt.* **14**, 2864 (1975).

²³P. W. Barber, *IEEE Trans. Microwave Theory Tech.* **25**, 373 (1977).

²⁴P. W. Barber, R. K. Chang, and H. Massoudi, to be published.

²⁵D.-S. Wang and M. Kerker, *Phys. Rev.* **24**, 1777 (1981).